

DAFTAR PUSTAKA

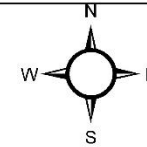
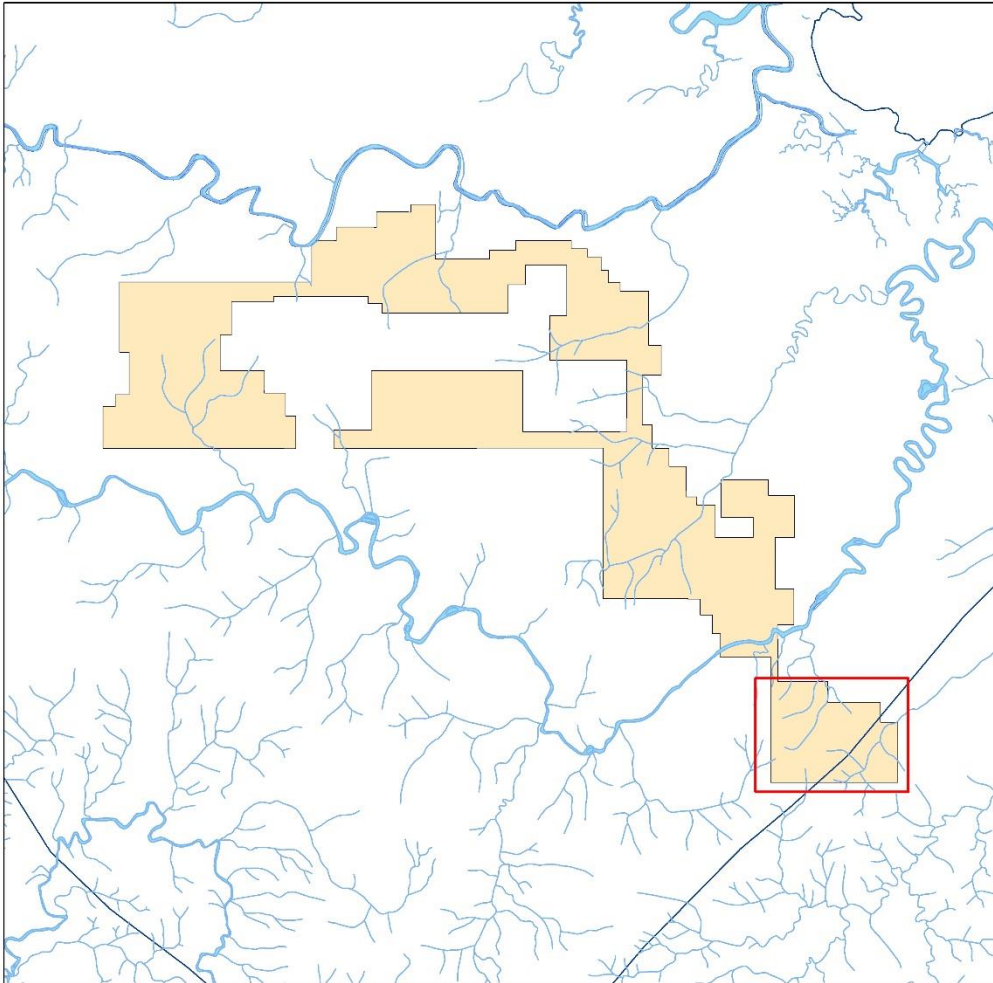
- Ahmad, W. 2006. *Nickel Laterites: Fundamental of Chemistry, Mineralogy, Weathering Processes, and Laterite Formation*, VALE Inco.
- Ahmad, W. 2008. *Nickel Laterites Fundamentals of Chemistry, Mineralogy, Weathering Processes, Formation, and Exploration*. VALE Inco.
- Astuti, W. 2012. Pembuatan Nickel Pig Iron (NPI) dari Bijih Nikel Laterit Indonesia Menggunakan *Mini Blast Furnace*. *Prosiding INSINAs*. Hal. 66-71.
- Burger, P. A. 1996. Origins and Characteristic of Lateritic Deposits. *Proseding nickel'96 the australisian institute of mining and metallurgy*. Hal. 179-183.
- Brand, N. W., Butt, C. R. & Elias, M., 1998. Nickel laterites: Classification and Features. *AGSO Journal of Australian Geology and Geophysics*, Volume 17, pp. 81-88..
- Boldt., 1967. Genesa Bahan Galian Bijih Nikel Laterit. *Indonesian Association of Geologist*. Bandung.
- Dalvi, A. D., Bacon, W. G. and Osborne, R.C. 2004. The Past and The Future of Nickel Laterites. *PDAC 2004 International Conference Trade Show and Investors Exchange, Toronto, Canada, March 7-10, Proceedings: Toronto, Canada, Prospectors and Developers Association of Canada*. Hal. 22-27.
- Golightly, J., 1979. Nickelferous Laterites: A General Description. *Journal of Electrostatics*, pp. 3-23.
- Golightly, J. P. (1981). Nickeliferous Laterite Deposits. *Economic Geology 75th Anniversary*, 710-735
- Hamilton, W. 1979. Tectonics of The Indonesian Region. *U. S. Geological Survey Profesional Paper*. Hal. 345.
- Hasria., Hasan, E.S., Deniyatno, Salihin, L.M.I. dan Asdiwam. 2020. *Characteristics of Ultramafic Igneous Rock Ophiolite Complex in Asera District, North Konawe Regency, Southeast Sulawesi Province, Indonesia*. *Journal of Geoscience, Engineering, Environment, and Technology*. 5(3), pp.108-112. <https://doi.org/10.25299/jgeet.2020.5.3.4113>
- Hutabarat, J. dan Ismawan. 2015. *Tinjauan Keterdapatan Batuan Ultramafik dalam Komplek Ophiolit Ciletuh di Daerah Ciletuh, Jawa Barat*. *Bulletin of Scientific Contribution: Geology*. 13(3), pp.213-220. <https://jurnal.unpad.ac.id/bsc/article/view/8408>
- Moore, E. M. 1992. *Structural Geology*. W. H. Freeman & Co : New York.

- Nahon, D. B., Boulange, B. & Colin, F., 1992. Metallurgy of Weathering: an Introduction, In Martini and Chesworth. *Weathering, Soil and Paleosols*, pp. 445-471.
- Parkinson, C. D., K. Miyazaki, K. Wakita, A.J. Barber, D.A. Carswell. 1998. An Overview and Tectonic Synthesis of The Pre-Tertiary Very-High-Pressure Metamorphic and Associated Rocks of Java, Sulawesi and Kalimantan, Indonesia, Island Arc. Hal. 184-200.
- Simandjuntak, T. O., Rusmana, E., Supandjono, J. B. dan Koswara, A. 1993. *Peta Geologi Lembar Bungku, Sulawesi, Skala 1:250.000*. Pusat Penelitian dan Pengembangan Geologi.
- Superiadi, A. 2007. *Processing Technology vs. Nickel Laterite Ore Characteristic, PT Inco*.
- Suratman. 2000. Geology of Laterite Nickel Deposit in Sorowako Area, South Sulawesi Province. *Indonesia in Proceedings of 29th Indonesia Association of Geologist*. Hal. 37-43.
- Surono, Simandjuntak, T. O. dan Rusmana, E., 1997. *Collision Mechanism Between The Oceanic and Continental Terranes in The Southeast Private Arm of Sulawesi, Eastern Indonesia*. *Bulletin Geology Research and Development Centre*. Hal. 109-125.
- Streckeisen, A. 1976. *To Each Plutonic Rock Its Proper Name*. *Earth Science Revision 12*, 1-33
- Trescases, J. J., 1975. *Levolution Geochimique Supergene des Roches Ultrabasiqes en Zone Tropicale; Formations des Gisements Nickeliferes de Nouvelle-Caledonie*. Paris, ORSTOM Mem. 78..
- Tonggiroh, Adi., 2009. Presisi Lapisan Endapan Nikel Laterit Berdasarkan Model Geokimia Batuan Ultramafik Daerah Sorowako Sulawesi Selatan. *Jurnal Penelitian Enjinerig Vol. 12, No. 2*. Fakultas Teknik Universitas Hasanuddin
- Yıldırım, H., Turan, A. and Yücel, O. 2012. Nickel Pig Iron (NPI) Production From Domestic Lateritic Nickel Ores Using Induction Furnace. *International Iron & Steel Symposium, Karabük, Türkiye*. Hal. 337-344.
- Waheed, A., 2002. *Nickel Laterites-A Short Course : Chemistry, Mineralogy, and Formation of Nickel Laterites* (tidak dipublikasikan). 212 h
- Waheed, A. 2009. *Nickel Laterites Fundamentals of Chemistry, Mineralogy, Weathering Processes, Formation, and Exploration*. VALE Inc

LAMPIRAN





LAMPIRAN A

PETA TUNJUK LOKASI



0 0.4 0.8 1.6 2.4 3.2 Miles

KETERANGAN

-  Sungai
-  Batas_Administrasi
-  Sungai_Utama
-  batas iup bumanik_geografis_



DEPARTEMEN TEKNIK PERTAMBANGAN
FAKULTAS TEKNIK
UNIVERSITAS HASANUDDIN
2022

TUGAS AKHIR
ANALISIS MINERALOGI DAN GEOKIMIA ENDAPAN NIKEL
LATERIT PIT C PT DJAVA BERKAH MINERAL JOB SITE
PT BUKIT MAKMUR ISTINDO NIKELTAMA

| | |
|---------------|--------------------------------------------------------------|
| DIGAMBAR OLEH | ANDI ARISKA D111171307 |
| PEMBIMBING I | Dr. Phil.nat. SRI WIDODO, ST, MT. NIP. 197101012012121001 |
| PEMBIMBING II | Dr. Ir. IRZAL NUR, MT. NIP : 196604091997031002 |

PETA TUNJUK LOKASI

| | |
|---------------|---------------|
| LAMPIRAN A | HALAMAN 56 |
|---------------|---------------|

LAMPIRAN B

HASIL DESKRIPSI MINERAL

No. Sayatan: 1
Lokasi : PIT C, PT Djava Berkah Mineral

Foto

| | A | B | C | D | E | F | G | H | I | J | | A | B | C | D | E | F | G | H | I | J | |
|----------|---|---|---|---|---|---|---|---|---|---|----------|---|---|---|---|---|---|---|---|---|---|----------|
| 1 | | | | | | | | | | | 1 | | | | | | | | | | | 1 |
| 2 | | | | | | | | | | | 2 | | | | | | | | | | | |
| 3 | | | | | | | | | | | 3 | | | | | | | | | | | |
| 4 | | | | | | | | | | | 4 | | | | | | | | | | | |
| 5 | | | | | | | | | | | 5 | | | | | | | | | | | |
| 6 | | | | | | | | | | | 6 | | | | | | | | | | | |

//- *Nikol*
Nikol

X-

Lensa Okuler : 10x
Perbesaran Total :50x

Lensa Obyektif : 5x

Tipe Batuan : Batuan Beku

Tipe Struktur : Masif

Mikroskopis :

Warna absorpsi abu-abu kecoklatan, warna interferensi abu-abu kehitaman, tekstur kristalinitashipokristalin, granularitas Faneritik, bentuk anhedral-subhedral, relasi inequigranular, komposisi mineral terdiri dari kuarsa, plagioklas, ortoklas, biotit dan muskovit.

Deskripsi Mineral

| Komposisi Mineral | Jumlah (%) | Keterangan Optik Mineral |
|--------------------------|-------------------|---------------------------------------------------------------------------------------------------------------------------------------------------------------------------------------------------------------------------------------------------------------------------------------------------------------------|
| Piroksen (Px) | 40 | Piroksin memiliki warna absorpsi transparan/ <i>colourless</i> , warna interferensi abu-abu kecoklatan. Memiliki relief sedang,intensitas sedang, memiliki belahan 2 arah, bentuk mineral anhedral-subhedral, ukuran 0,01 mm-0,5 mm, tidak memiliki kembaran pecahan uneven, sudut gelap 47.5°, jenis gelap miring. |
| Olivin (Ol) | 35 | Olivin memiliki warna absorpsi transparan/ <i>colourless</i> warna interferensi biru kehijauan, relief sedang intensitas sedang bentuk anhedral-subhedral ukuran 0,06 mm-0,2 mm pecahan uneven tidak memiliki belahan sudut gelap 47° gelap miring. |

| | | |
|-----------------------|-----------|-----------------------------------------------------------------------------------------------------------------------------------------------------------------------------------------------------------------------------------------------------------------------------|
| Serpentin (Sp) | 15 | Serpentin memiliki warna absorbsi transparan/ <i>colourless</i> , warna interferensi putih keabuan relief sedang, intensitas sedang, tidak memiliki belahan tidak memiliki pecahan, bentuk anhedral-subhedral ukuran 0.02 – 0.5 mm sudut gelapan 40 ° jenis gelapan miring. |
| Klorit (Cl) | 10 | Memiliki warna absorpsi hijau, bentuk anhedral-subhedral, relief rendah, intensitas kuat, pleokroisme kuat, ukuran mineral 0,2 mm, warna interferensi hijau, tidak memiliki kembaran, jenis gelapan miring 25°. |

LAMPIRAN C

HASIL ANALISIS *X-RAY DIFFRACTION* (XRD)

Match! Phase Analysis Report

Sample: LIM-PIT-C (5-70)

Sample Data

| | |
|-------------------------------|------------------------------------------------|
| File name | LIM-PIT-C.RAW |
| File path | D:/ika/ika/XRD IKA TAMBANG/LIM-PIT-C/LIM-PIT-C |
| Data collected | Dec 13, 2022 13:34:25 |
| Data range | 5.020° - 70.020° |
| Original data range | 5.000° - 70.000° |
| Number of points | 3251 |
| Step size | 0.020 |
| Rietveld refinement converged | No |
| Alpha2 subtracted | No |
| Background subtr. | No |
| Data smoothed | Yes |
| 2theta correction | 0.02° |
| Radiation | X-rays |
| Wavelength | 1.540600 Å |

Matched Phases

| <i>Inde</i> <i>x</i> | <i>Amount</i> <i>(%)</i> | <i>Name</i> | <i>Formula sum</i> |
|-------------------------|-----------------------------|-------------------------------|--------------------|
| A | 37.9 | Goethite | Fe H O2 |
| B | 26.7 | Talc | H2 Mg3 O12 Si4 |
| C | 26.4 | Chlorite | H4 Mg3 O9 Si2 |
| D | 4.6 | Magnetite | Fe3 O4 |
| E | 4.5 | Maghemite | Fe2 O3 |
| | 7.9 | <i>Unidentified peak area</i> | |

Amounts calculated by RIR (Reference Intensity Ratio) method

Elemental composition of sample (identified crystalline phases only)

Element Amount (weight %)

| | |
|-----------------|---------------|
| O | 43.46% |
| Fe | 30.28% |
| Si | 13.24% |
| Mg | 12.06% |
| H | 0.96% |
| <i>LE (sum)</i> | <i>44.42%</i> |

Matching entry details

A: Goethite (37.9 %)*

| | |
|------------------------|-------------------------------------|
| Formula sum | Fe H O2 |
| Entry number | 96-900-2159 |
| Figure-of-Merit (FoM) | 0.707083* |
| Total number of peaks | 182 |
| Peaks in range | 32 |
| Peaks matched | 13 |
| Intensity scale factor | 0.83* |
| Space group | P n m a |
| Crystal system | orthorhombic |
| Unit cell | a= 9.9134 Å b= 3.0128 Å c= 4.5800 Å |
| I/Ic | 2.57 |
| Calc. density | 4.314 g/cm ³ |

| | |
|------------------------------|-----------------------------------------------------------------------------------------------------------------------------------------------------------------------------------------------------------|
| Reference | Gualtieri A., Venturelli P., "In situ study of the goethite-hematite phase transformation by real timesynchrotron powder diffractionSample at T = 25 C", American Mineralogist 84 , 895-904 (1999) |
| | |
| <i>B: Talc (26.7 %)*</i> | |
| Formula sum | H2 Mg3 O12 Si4 |
| Entry number | 96-900-8298 |
| Figure-of-Merit (FoM) | 0.625052* |
| Total number of peaks | 251 |
| Peaks in range | 167 |
| Peaks matched | 38 |
| Intensity scale factor | 0.24* |
| Space group | C -1 |
| Crystal system | triclinic (anorthic) |
| Unit cell | a= 5.2900 Å b= 9.1730 Å c= 9.4600 Å α= 90.460° β= 98.680 ° γ= 90.090 ° |
| I/Ic | 1.03 |
| Calc. density | 2.776 g/cm ³ |
| Reference | Perdikatsis B., Burzlaff H., "Strukturverfeinerung am talk Mg3[(OH)2Si4O10]", Zeitschrift fur Kristallographie 156 , 177-186 (1981) |
| | |
| <i>C: Chlorite (26.4 %)*</i> | |
| Formula sum | H4 Mg3 O9 |
| Entry number | 96-900-0159 |
| Figure-of-Merit (FoM) | 0.659152* |
| Total number of peaks | 91 |
| Peaks in range | 91 |
| Peaks matched | 23 |
| Intensity scale factor | 0.18* |
| Space group | C 1 |
| Crystal system | triclinic (anorthic) |
| Unit cell | a= 5.3350 Å b= 9.2400 Å c= 28.7350 Å α= 90.000° β= 90.000 ° γ= 90.000 ° |
| I/Ic | 0.81 |
| Calc. density | 2.599 g/cm ³ |
| Reference | Lister J. S., Bailey S. W., "Chlorite polytypism: IV. Regular two-layer structuresrefined structure", American Mineralogist 52 , 1614-1631 (1967) |

*D: Magnetite (4.6 %)**

| | |
|------------------------|------------------------------------------------------------------------------------------------------------------------------------------------------------------------------------------------------------------------------------------------------------------|
| Formula sum | Fe ₃ O ₄ |
| Entry number | 96-900-2331 |
| Figure-of-Merit (FoM) | 0.615835* |
| Total number of peaks | 34 |
| Peaks in range | 9 |
| Peaks matched | 5 |
| Intensity scale factor | 0.22* |
| Space group | F d -3 m |
| Crystal system | cubic |
| Unit cell | a= 8.1177 Å |
| I/Ic | 5.68 |
| Calc. density | 5.750 g/cm ³ |
| Reference | Haavik C., Stolen S., Fjellvag H., Hanfland M., Hausermann D., "Equation of state of magnetite and its high- pressure modification: Thermodynamics of the Fe-O system at high pressure Sample at P = 26.9 GPa", American Mineralogist 85 , 514-523 (2000) |

*E: Maghemite (4.5 %)**

| | |
|------------------------|-------------------------------------------------------------------------------------------------------------------------------------------------------------------------------------------------------------------------------------|
| Formula sum | Fe ₂ O ₃ |
| Entry number | 96-901-2693 |
| Figure-of-Merit (FoM) | 0.566507* |
| Total number of peaks | 393 |
| Peaks in range | 77 |
| Peaks matched | 13 |
| Intensity scale factor | 0.14* |
| Space group | P 43 21 2 |
| Crystal system | tetragonal |
| Unit cell | a= 8.3396 Å c= 8.3220 Å |
| I/Ic | 3.62 |
| Calc. density | 4.887 g/cm ³ |
| Reference | Greaves C., "A powder neutron diffraction investigation of vacancy ordering and covalence in gamma-Fe ₂ O ₃ Locality: synthetic Sample: T = 4 K", Journal of Solid State Chemistry 49 , 325-333 (1983) |

() 2theta values have been shifted internally for the calculation of the amounts, the intensity scaling factors as well as the figure-of-merit (FoM), due to the active search-match option 'Automatic zero point adaption'.*

Candidates

| Name | Formula | Entry No. | FoM |
|--------------------------------------------------------------------------------------------------------------------------------------------------------------------------------------------------------|--------------------------------------------------------------------------------------------------------------------------------------------------------------------------|------------------|------------|
| (Mo ₄ Pt) _{1.6} | Mo _{6.4} Pt _{1.6} | 96-210-7217 | 0.7444 |
| Ir ₂ (Nb V) ₃ | Ir ₂ Nb ₃ V ₃ | 96-152-3138 | 0.7443 |
| (Mo _{0.8} Pt _{0.2}) | Mo _{0.8} Pt _{0.2} | 96-152-3629 | 0.7441 |
| (Mo ₁₇ Pt ₃) _{0.4} | Mo _{6.8} Pt _{1.2} | 96-153-9144 | 0.7419 |
| | Sn V ₃ | 96-152-7072 | 0.7418 |
| | Sn V ₃ | 96-154-0205 | 0.7355 |
| Britvinite | C ₂ B _{3.468} F ₂ Mg ₉ O ₅₈ Pb _{14.144} Si _{10.532} | 96-901-2669 | 0.7262 |
| | Ir Ti ₃ | 96-153-7944 | 0.7234 |
| Barium | Ba | 96-900-8529 | 0.7213 |
| (Mo _{0.7} Re _{0.3}) | Mo _{0.7} Re _{0.3} | 96-152-2723 | 0.7211 |
| | Mo ₃ Os | 96-152-2995 | 0.7198 |
| | Mo ₃ Os | 96-210-6125 | 0.7185 |
| Gyrolite | Al Ca ₁₆ H ₂₈ Na O ₈₂ Si ₂₃ | 96-900-9473 | 0.7123 |
| Dirubidium copper hexacyanoferrate(II) | C ₆ Cu Fe N ₆ Rb ₂ | 96-101-0365 | 0.7106 |
| | Ir Ti ₃ | 96-153-7951 | 0.7098 |
| Richetite | Fe _{0.47} H ₂₄ Mg _{0.83} O ₁₇₃ Pb _{8.74} U ₃₆ | 96-900-4468 | 0.7024 |
| Okenite | Ca ₅ H ₂₃ O ₃₂ Si ₉ | 96-900-0884 | 0.7011 |
| Okenite | Ca ₅ H ₁₈ O ₃₂ Si ₉ | 96-901-5623 | 0.7011 |
| Ag ₃ S I | Ag ₃ I S | 96-151-0009 | 0.6978 |
| Na (Cl O ₄) | Cl Na O ₄ | 96-722-3700 | 0.6963 |
| Litharge | O Pb | 96-901-2697 | 0.6892 |
| | Nb P ₂ S ₈ | 96-153-4699 | 0.6881 |
| Charoite | Ba _{0.16} Ca _{12.82} F H _{4.18} K _{6.94} Mn _{0.18} Na _{3.18} O _{92.59} Si ₃₅ Sr _{0.5} | 96-901-6709 | 0.6847 |
| | Ca ₈ H ₁₂ O ₂₉ P ₆ | 96-153-4328 | 0.6840 |
| Ca ₈ H ₂ (P O ₄) ₆ (H ₂ O) ₅ | Ca P ₆ O ₂ | 96-153-4328 | 0.6840 |
| Calcium Catena-polyphosphat C ₁₈ H ₃₆ N ₄ I ₁₀ Pb ₃ | C ₁₈ H ₃₆ I ₁₀ N ₄ Pb ₃ | 96-724-1117 | 0.6814 |
| beryllium bis(hypophosphite) | Be H ₄ O ₄ P ₂ | 96-201-4099 | 0.6792 |
| Copper diniobate | Cu Nb ₂ O ₆ | 96-100-6091 | 0.6787 |
| Zn Se | Se Zn | 96-153-8614 | 0.6784 |
| | Ag Cr O ₂ | 96-720-9333 | 0.6776 |
| | C _{49.05} Cl _{0.42} F _{21.89} O _{0.21} | 96-403-2118 | 0.6755 |
| | C ₁₀ H ₁₀ F ₆ N O ₁₀ P | 96-770-0269 | 0.6730 |
| Dipotassium copper hexacyanoferrate(II) | C ₆ Cu Fe K ₂ N ₆ | 96-101-0360 | 0.6723 |
| | C ₁₁₁ N ₅ O ₁₂ Se ₅ Sn ₄ | 96-722-3367 | 0.6711 |
| | H _{7.5} I _{0.5} Lu ₂ O _{6.5} | 96-703-1395 | 0.6706 |
| Silicon carbide (Moissanite 3C) | Si C | 96-101-0996 | 0.6705 |
| Dysprosium | Dy | 96-900-8495 | 0.6705 |
| | C Si | 96-900-8857 | 0.6705 |
| U ₃₀ | Li Mg ₄ O ₂₃₉ U ₃₀ | 96-702-5955 | 0.6699 |
| ((Mg Al) (Si ₄ O ₁₀ (H ₂ O) ₂ (O H))) (H ₂ O) _{1.46} (C ₁₆ N ₂ O ₂ H ₁₀) _{0.045} | C _{0.72} H _{8.37} Al Mg N _{0.09} O _{14.55} Si ₄ | 96-153-3370 | 0.6693 |
| | Cs ₄ Se ₄ Si | 96-810-1314 | 0.6682 |
| bismuth cadmium oxide phosphate | Bi _{15.32} Cd ₁₀ O ₅₈ P ₁₀ | 96-433-2414 | 0.6678 |
| | C ₃₀ H ₆₁ N ₉ O ₂₆ Pt ₃ | 96-200-9381 | 0.6675 |
| | C _{82.5} H _{10.5} F ₁₆ | 96-705-3323 | 0.6673 |
| Ashcroftine-(Y) | C ₁₆ H _{14.8} K _{10.4} Na _{8.26} O _{202.96} Si _{54.16} Y ₂₄ | 96-900-1108 | 0.6673 |
| Zn Mn ₃ O ₇ (H ₂ O) ₃ | H ₆ Mn ₃ O ₁₀ Zn | 96-231-0846 | 0.6671 |
| propane-1,3-diammonium bis(zinc phosphate) | C _{1.875} H _{7.5} N _{1.25} O ₅ P _{1.25} Zn _{1.25} | 96-220-0281 | 0.6670 |
| Nb N | N _{0.77} Nb | 96-154-0243 | 0.6668 |
| Pb O | O Pb | 96-153-3610 | 0.6665 |
| beta-Na ₃ PS ₄ | Na ₃ P S ₄ | 96-722-9734 | 0.6659 |
| | C ₁₄ N ₆ O ₅ W | 96-407-9201 | 0.6658 |
| | Cu Fe K O ₈ P ₂ | 96-156-3290 | 0.6657 |

and 5344 others...

Search-Match

Settings

| | |
|--------------------------------------------|----------------------|
| Reference database used | COD-Inorg 2021.06.14 |
| Automatic zeropoint adaptation | Yes |
| Downgrade entries with low scaling factors | Yes |
| Minimum figure-of-merit (FoM) | 0.60 |
| 2theta window for peak corr. | 0.30 deg. |
| Minimum rel. int. for peak corr. | 1 |
| Parameter/influence 2theta | 0.50 |
| Parameter/influence intensities | 0.50 |
| Parameter multiple/single phase(s) | 0.50 |

Criteria for entries added by user

Reference:

Entry number: 96-201-4618;96-201-4619;96-201-4931;96-220-5377;96-220-7380;96-220-7381;96-900-0159;96-900-4189;96-901-0164;96-901-0165;96-901-0166;96-901-0167;96-901-0168;96-901-0169;96-901-0170;96-101-1153;96-300-0049;96-900-8041;96-900-8298;96-900-8732;96-901-4436;96-900-1115;96-900-6317;96-900-6318;96-900-6319;96-901-2693;96-100-8767;96-100-8768;96-100-8769;96-101-1088;96-221-1653;96-900-2159;96-900-2160;96-900-3077;96-900-3078;96-900-3079;96-900-3080;96-900-3081;96-901-0407;96-901-0408;96-901-0409;96-901-0410;96-901-0411;96-901-1413;96-901-5697;96-901-6060;96-901-6179;96-901-6407;96-101-1033;96-101-1085;96-722-8111;96-900-0927;96-900-0928;96-900-0929;96-900-0930;96-900-0931;96-900-0932;96-900-0933;96-900-0934;96-900-0935;96-900-2317;96-900-2318;96-900-2319;96-900-2320;96-900-2321;96-900-2322;96-900-2323;96-900-2324;96-900-2325;96-900-2326;96-900-2327;96-900-2328;96-900-2329;96-900-2330;96-900-2331;96-900-2332;96-900-2333;96-900-2674;96-900-2675;96-900-4088;96-900-4156;96-900-4157;96-900-5813;96-900-5814;96-900-5815;96-900-5816;96-900-5817;96-900-

5837;96-900-5838;96-900-5839;96-900-5840;96-900-5841;96-900-5842;96-900-5843;96-900-6185;96-900-6190;96-900-6195;96-900-6200;96-900-6243;96-900-6248;96-900-6253;96-900-6266;96-900-6921;96-900-6922;96-900-7645;96-900-7707;96-900-7708;96-900-9769;96-900-9770;96-901-0940;96-901-0941;96-901-0942;96-901-3530;96-901-3531;96-901-3532;96-901-3533;96-901-3534;96-901-3535;96-901-3536;96-101-1098;96-101-1160;96-101-1173;96-101-1177;96-101-1201;96-110-0020;96-500-0036;96-900-0776;96-900-0777;96-900-0778;96-900-0779;96-900-0780;96-900-0781;96-900-5018;96-900-5019;96-900-5020;96-900-5021;96-900-5022;96-900-5023;96-900-5024;96-900-5025;96-900-5026;96-900-5027;96-900-5028;96-900-5029;96-900-5030;96-900-5031;96-900-5032;96-900-5033;96-900-5034;96-900-7379;96-900-8093;96-900-8094;96-900-9667;96-901-0145;96-901-0146;96-901-0147;96-901-1494;96-901-1495;96-901-1496;96-901-1497;96-901-2601;96-901-2602;96-901-2603;96-901-2604;96-901-2605;96-901-2606;96-901-3322;96-901-5023;96-101-1241;96-101-1268;96-210-8028;96-210-8029;96-591-0083;96-900-0140;96-900-2161;96-900-2162;96-900-2163;96-900-9783;96-901-4881;96-901-5066;96-901-5504;96-901-5965;96-901-6458;96-101-1046;96-155-0599;96-900-9231;96-900-9235;96-901-5000;96-100-1742;96-100-1744;96-101-0918;96-101-0929;96-101-0963;96-210-0993;96-591-0096;96-721-4218;96-721-4219;96-900-0096;96-900-0575;96-900-0966;96-900-0967;96-900-0968;96-900-0969;96-900-0970;96-900-0971;96-900-1298;96-900-1299;96-900-7287;96-900-7688;96-900-7690;96-900-9668;96-900-9669;96-900-9866;96-901-2074;96-901-3466;96-901-4217;96-901-4345;96-901-4393;96-901-4416;96-901-4525;96-901-4612;96-901-4745;96-901-4773;96-901-

4878;96-901-4892;96-901-5067;96-901-5074;96-901-5391;96-901-5461;96-901-5482;96-901-5488;96-901-5692;96-901-5762;96-901-5836;96-901-6021;96-901-6023;96-901-6180;96-901-6201;96-901-6465;96-901-6706;96-901-6707;96-900-1591;96-150-5105;96-154-0680;96-101-1082;96-120-0017;96-154-4376;96-900-3875;96-900-8238;96-901-1748;96-901-5516;96-901-5977;96-900-0097;96-900-0381;96-900-0972;96-900-0973;96-900-0974;96-900-0975;96-900-0976;96-900-1850;96-900-1851;96-900-1852;96-900-1853;96-900-1854;96-900-1855;96-900-2811;96-900-2812;96-900-2813;96-900-2814;96-900-2815;96-900-2816;96-900-2817;96-900-2818;96-900-2819;96-900-2820;96-900-2821;96-900-7693;96-900-9130;96-901-0201;96-901-0202;96-901-0203;96-901-0209;96-901-0210;96-901-0211;96-901-0214;96-901-0215;96-901-0216;96-901-0217;96-901-0218;96-901-0224;96-901-0225;96-901-0226;96-901-0227;96-901-1208

Peak List

| <i>N</i> <i>o.</i> | <i>2theta</i> [°] | <i>d</i> [Å] | <i>I/I0</i> (peak height) | <i>Counts</i> (peak area) | <i>FWHM</i> | <i>Matche</i> <i>d</i> |
|-----------------------|----------------------|--------------|------------------------------|------------------------------|-------------|---------------------------|
| 1 | 9.60 | 9.2055 | 340.29 | 13.98 | 0.4400 | B |
| 2 | 12.48 | 7.0869 | 522.40 | 21.46 | 0.4400 | C |
| 3 | 18.80 | 4.7163 | 498.00 | 22.32 | 0.4800 | B,C,D |
| 4 | 19.94 | 4.4492 | 206.65 | 20.84 | 1.0800 | C |
| 5 | 21.36 | 4.1565 | 1000.00 | 89.64 | 0.9600 | A,B,C,E |
| 6 | 25.12 | 3.5422 | 651.73 | 21.91 | 0.3600 | B |
| 7 | 26.72 | 3.3336 | 596.36 | 22.27 | 0.4000 | A,C |
| 8 | 28.72 | 3.1059 | 978.28 | 29.23 | 0.3200 | B |
| 9 | 31.54 | 2.8343 | 164.85 | 4.93 | 0.3200 | C |
| 10 | 33.26 | 2.6916 | 481.98 | 25.20 | 0.5600 | A |
| 11 | 34.86 | 2.5716 | 371.60 | 23.59 | 0.6800 | A,B,C |
| 12 | 35.86 | 2.5022 | 741.67 | 77.56 | 1.1200 | A,B,C,E |
| 13 | 36.84 | 2.4378 | 971.21 | 87.06 | 0.9600 | A,B,C,D |
| 14 | 40.32 | 2.2351 | 237.36 | 19.50 | 0.8800 | A,B,C,E |
| 15 | 41.34 | 2.1822 | 174.87 | 24.17 | 1.4800 | A,B |
| 16 | 44.34 | 2.0413 | 602.75 | 15.76 | 0.2800 | B,C,D |
| 17 | 53.66 | 1.7067 | 385.10 | 38.83 | 1.0800 | A,B,E |
| 18 | 59.12 | 1.5614 | 215.46 | 11.27 | 0.5600 | A,B,D |
| 19 | 60.22 | 1.5355 | 177.55 | 17.90 | 1.0800 | B |
| 20 | 61.96 | 1.4965 | 189.40 | 19.10 | 1.0800 | A,B |
| 21 | 63.20 | 1.4701 | 136.45 | 34.66 | 2.7200 | A,B,E |
| 22 | 65.06 | 1.4325 | 164.83 | 7.39 | 0.4800 | B,D,E |

Integrated Profile Areas

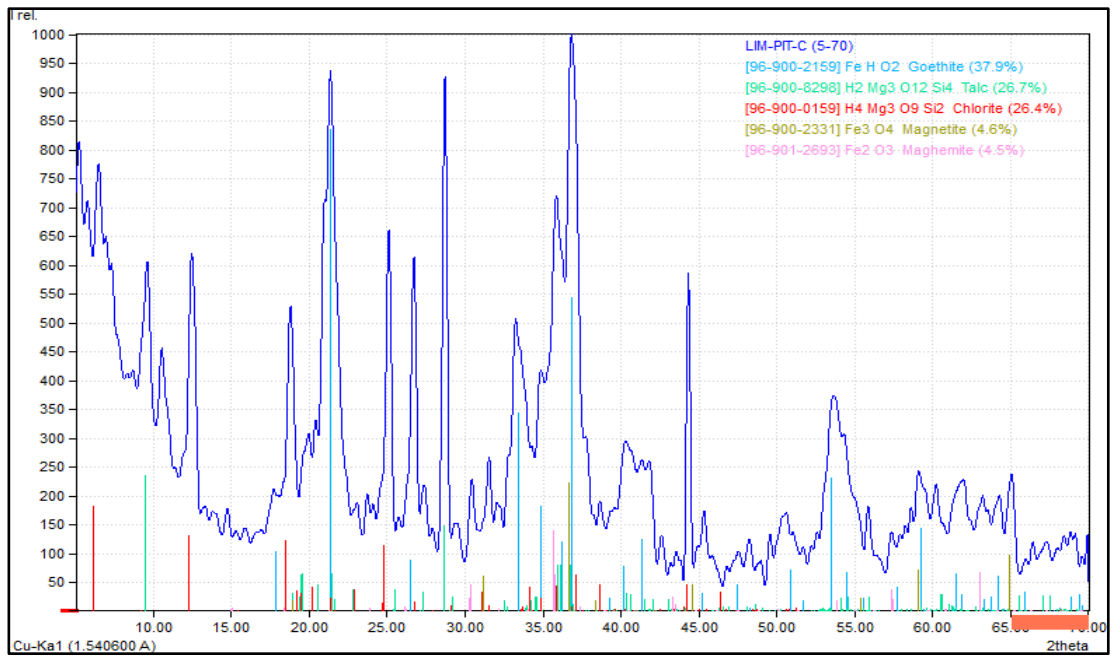
Based on calculated profile

| <i>Profile area</i> | <i>Counts</i> | <i>Amount</i> |
|-----------------------------------------|---------------|---------------|
| Overall diffraction profile | 74859 | 100.00% |
| Background radiation | 41559 | 55.52% |
| Diffraction peaks | 33300 | 44.48% |
| Peak area belonging to selected phases | 27365 | 36.56% |
| <i>Peak area of phase A (Goethite)</i> | <i>13051</i> | <i>17.43%</i> |
| <i>Peak area of phase B (Talc)</i> | <i>6225</i> | <i>8.32%</i> |
| <i>Peak area of phase C (Chlorite)</i> | <i>4317</i> | <i>5.77%</i> |
| <i>Peak area of phase D (Magnetite)</i> | <i>1830</i> | <i>2.44%</i> |
| <i>Peak area of phase E (Maghemite)</i> | <i>1942</i> | <i>2.59%</i> |
| Unidentified peak area | 5935 | 7.93% |

Peak Residuals

| <i>Peak data</i> | <i>Counts</i> | <i>Amount</i> |
|---------------------------------------------|---------------|---------------|
| Overall peak intensity | 649 | 100.00% |
| Peak intensity belonging to selected phases | 361 | 55.62% |
| Unidentified peak intensity | 288 | 44.38% |

Diffraction Pattern Graphics



Match! Copyright © 2003-2021 CRYSTAL IMPACT, Bonn, Germany

Match! Phase Analysis Report

Sample: SAP-PIT-C (5-70)

Sample Data

| | |
|-------------------------------|------------------------------------------------|
| File name | SAP-PIT-C.RAW |
| File path | D:/ika/ika/XRD IKA TAMBANG/SAP-PIT-C/SAP-PIT-C |
| Data collected | Dec 13, 2022 13:34:26 |
| Data range | 5.000° - 70.000° |
| Original data range | 5.000° - 70.000° |
| Number of points | 3251 |
| Rietveld refinement converged | No |
| Step size | 0.020 |
| Background subtr. | No |
| Data smoothed | Yes |
| Radiation | X-rays |
| Wavelength | 1.540600 Å |

Matched Phases

| Inde x | Amount (%) | Name | Formula sum |
|-------------------|-----------------------|-------------------------------|------------------------|
| A | 36.2 | Antigorite | H58 Mg45 O138 Si32 |
| B | 29.5 | Goethite | Fe H O2 |
| C | 20.3 | Lizardite | H4 Mg3 O9 Si2 |
| D | 10.8 | Talc | H2 Mg3 O12 Si4 |
| E | 3.3 | Enstatite | Fe0.41 Mg0.59 O3 Si |
| | <i>13.9</i> | <i>Unidentified peak area</i> | |

Amounts calculated by RIR (Reference Intensity Ratio) method

Elemental composition of sample (identified crystalline phases only)

| Element Amount (weight %) | |
|---------------------------|---------------|
| O | 47.43% |
| Fe | 18.56% |
| Mg | 17.74% |
| Si | 16.14% |
| H | 1.18% |
| <i>LE (sum)</i> | <i>48.61%</i> |

Matching entry details

A: Antigorite (36.2 %)*

| | |
|------------------------|-------------------------------------------------------------------------------------------------------------------------------------------------------------------------------------------|
| Formula sum | H58 Mg45 O138 Si32 |
| Entry number | 96-900-4000 |
| Figure-of-Merit (FoM) | 0.626451* |
| Total number of peaks | 327 |
| Peaks in range | 327 |
| Peaks matched | 54 |
| Intensity scale factor | 0.24* |
| Space group | C 1 2/m 1 |
| Crystal system | monoclinic |
| Unit cell | a= 81.6640 Å b= 9.2550 Å c= 7.2610 Å β= |
| 91.409 ° | |
| I/Ic | 0.70 |
| Calc. density | 2.578 g/cm ³ |
| Reference | Capitani G. C., Mellini M., "The crystal structure of a second antigorite polysome (m = 16), by single-crystal synchrotron diffraction", American Mineralogist 91 , 394-399 (2006) |

B: Goethite (29.5 %)*

| | |
|------------------------|-------------------------------------|
| Formula sum | Fe H O2 |
| Entry number | 96-900-2159 |
| Figure-of-Merit (FoM) | 0.657432* |
| Total number of peaks | 182 |
| Peaks in range | 182 |
| Peaks matched | 10 |
| Intensity scale factor | 0.72* |
| Space group | P n m a |
| Crystal system | orthorhombic |
| Unit cell | a= 9.9134 Å b= 3.0128 Å c= 4.5800 Å |
| I/Ic | 2.57 |
| Calc. density | 4.314 g/cm ³ |

| | |
|------------------------|-----------------------------------------------------------------------------------------------------------------------------------------------------------------------------------------------------------|
| Reference | Gualtieri A., Venturelli P., "In situ study of the goethite-hematite phase transformation by real timesynchrotron powder diffractionSample at T = 25 C", American Mineralogist 84 , 895-904 (1999) |
| C: Lizardite (20.3 %)* | |
| Formula sum | H4 Mg3 O9 Si2 |
| Entry number | 96-900-0849 |
| Figure-of-Merit (FoM) | 0.551063* |
| Total number of peaks | 112 |
| Peaks in range | 112 |
| Peaks matched | 7 |
| Intensity scale factor | 0.26* |
| Space group | P 3 1 m |
| Crystal system | trigonal (hexagonal axes) |
| Unit cell | a= 5.3320 Å c= 7.2330 Å |
| I/Ic | 1.35 |
| Calc. density | 2.584 g/cm ³ |
| Reference | Mellini M., "The crystal structure of lizardite 1T: hydrogen bonds and polytypism", American Mineralogist 67 , 587-598 (1982) |
| D: Talc (10.8 %)* | |
| Formula sum | H2 Mg3 O12 Si4 |
| Entry number | 96-900-8041 |
| Figure-of-Merit (FoM) | 0.589295* |
| Total number of peaks | 298 |
| Peaks in range | 298 |
| Peaks matched | 32 |
| Intensity scale factor | 0.11* |
| Space group | C 1 2/c 1 |
| Crystal system | monoclinic |

| | |
|------------------------|---------------------------------------------------------------------------------------------------------------------------------------------------------------------|
| Unit cell 100.000 ° | a= 5.2600 Å b= 9.1000 Å c= 18.8100 Å β= |
| I/Ic | 1.05 |
| Calc. density | 2.841 g/cm ³ |
| Reference | Gruner J. W., "The crystal structures of talc and pyrophylliteLocality: Harford County, Maryland, USA", Zeitschrift fur Kristallographie 88 , 412-419 (1934) |

E: Enstatite (3.3 %)*

| | |
|------------------------|-------------------------------------------------------------------------------------------------------------------------------------------------------------------------------------------------------------------------------|
| Formula sum | Fe0.41 Mg0.59 O3 Si |
| Entry number | 96-900-6428 |
| Figure-of-Merit (FoM) | 0.576745* |
| Total number of peaks | 500 |
| Peaks in range | 500 |
| Peaks matched | 22 |
| Intensity scale factor | 0.02* |
| Space group | P b c a |
| Crystal system | orthorhombic |
| Unit cell | a= 18.2974 Å b= 8.9040 Å c= 5.2092 Å |
| I/Ic | 0.63 |
| Calc. density | 3.548 g/cm ³ |
| Reference | Hugh-Jones D A, Chopelas A., Angel R. J., "Tetrahedral compression in (Mg,Fe)SiO ₃ orthopyroxenesSample: P = 0.00 GPa, synthetic En60 orthopyroxene", Physics and Chemistry of Minerals 24 , 301-310 (1997) |

()2theta values have been shifted internally for the calculation of the amounts, the intensity scaling factors as well as the figure-of-merit (FoM), due to the active search-match option 'Automatic zero point adaption'.*

Candidates

| Name | Formula | Entry No. | FoM |
|----------------------------------------------------------------------------|---------------------------------------------------------------------------------------|------------------|------------|
| Ba3 (P Mo12 O40)2 (D2 O)55.3 | Mo24 O113.6 P2 | 96-153-3530 | 0.7382 |
| H3 (P Mo12 O40) (H2 O)6 | H15 Mo12 O46 P | 96-210-6186 | 0.6823 |
| | C7 F N O7 P2 Zr | 96-723-8536 | 0.6688 |
| | O69 P W12 | 96-901-5518 | 0.6645 |
| | H61 O69 P W12 | 96-101-0634 | 0.6627 |
| Trihydrogen dodecatungstophosphate hydrate(29) | | | |
| Pd21 Ti50 Si100 Al92 O384 | Al92 O384 Pd21 Si100 Ti50 | 96-152-7030 | 0.6606 |
| | Cs11.5 K1.5 Na1.5 O134 Si3 Ti10 W27 | 96-430-6277 | 0.6605 |
| Pd18 Ti56 (Si100 Al92 O384) | Al92 O384 Pd18 Si100 Ti56 | 96-152-7029 | 0.6523 |
| (Cs45.3 Na46.7) (Al92 Si100 O384) | Al92 Cs45.3 Na46.7 O384 Si100 | 96-153-3075 | 0.6496 |
| Cs27.49 Na60.88 (Al88 Si104 O384) (H2 O)18.72 | Al88 Cs27.49 H37.44 Na60.88 O402.72 Si104 | 96-152-1411 | 0.6486 |
| | C4 N Nd O11 P2 S | 96-400-3143 | 0.6483 |
| Ag23 Ti69 (Al92 Si100 O384) | Ag23 Al92 O384 Si100 Ti69 | 96-150-9758 | 0.6435 |
| | Ni2 Sc Si2 | 96-153-9239 | 0.6404 |
| Rhombochase | Fe H9 O12 S2 | 96-901-3792 | 0.6397 |
| Cs44.8 Na54.4 (Al96 Si96 O384) | Al96 Cs44.8 Na54.4 O384 Si96 | 96-154-0967 | 0.6390 |
| (Ag0.76 Mg0.24)2 Ca | Ag1.48 Ca Mg0.52 | 96-150-9597 | 0.6389 |
| Fencooperite | C2 H1.38 Ba6 Cl1.62 Fe3 O31.38 Si8 | 96-900-4632 | 0.6317 |
| | B Cl2 H4 N O3 Zn2 | 96-400-3328 | 0.6313 |
| Okenite | Ca5 H23 O32 Si9 | 96-900-0884 | 0.6312 |
| Okenite | Ca5 H18 O32 Si9 | 96-901-5623 | 0.6312 |
| In2.42 Al22 O34.8 | Al22 In2.42 O34.8 | 96-153-6597 | 0.6304 |
| Cd3 Al2 Si3 O12 | Al2 Cd3 O12 Si3 | 96-153-8398 | 0.6296 |
| beryllium bis(hypophosphite) | Be H4 O4 P2 | 96-201-4099 | 0.6290 |
| | C6 H11 S Ti | 96-403-0499 | 0.6286 |
| Diaoyudaosite | Al11 Cd0.105 Na1.008 O17.111 | 96-901-1272 | 0.6279 |
| Ca Br2 | Br2 Ca | 96-403-1228 | 0.6278 |
| catena-(octakis(2-Methylpiperidinium) 96-410-2795 0.6278 | C48 H112 Ga14 N8 Se33 Sn2 Zn4 | 96-900-0736 | 0.6275 |
| tritriaconta-selenido- tetradeca-gallium-tetra-zinc-di-tin) | | | |
| | Fe2 O4 Si | 96-900-6926 | 0.6274 |
| Nd Ga3 (B O3)4 | B4 Ga3 Nd O12 | 96-151-1742 | 0.6273 |
| Fayalite | Fe2.001 O4 Si0.999 | 96-900-0396 | 0.6272 |
| | Fe2 O4 Si | 96-900-5823 | 0.6270 |
| | C5 H13 N O44 Si22 | 96-154-6305 | 0.6263 |
| Picropharmacolite | As4 Ca4 H24 Mg O27 | 96-900-0812 | 0.6263 |
| Lithium Manganese(III) Manganese(IV) Oxide | Li Mn2 O4 | 96-151-3968 | 0.6258 |
| diammonium tetrabromocuprate dihydrate | Br4 Cu H12 N2 O2 | 96-721-4573 | 0.6257 |
| Tm0.524 Al0.58 B14 | Al0.58 B14 Tm0.524 | 96-154-0307 | 0.6254 |
| (Zn4 In16 S33) ((N2 C4 H8) ((N H2) C3 H6)2) | In16 S33 Zn4 | 96-412-3978 | 0.6250 |
| | Ge4 K4 Li2 O13 Ti | 96-400-3457 | 0.6249 |
| | Eu2 O7 Ta2 | 96-901-5256 | 0.6246 |
| Richelsdorffite | As4 Ca2 Cl Cu5 H18 O28 Sb | 96-901-1487 | 0.6245 |
| | C102 B2 N2 | 96-413-5311 | 0.6244 |
| Ho.63 Al.74 B14 | Al0.74 B14 Ho0.63 | 96-153-8906 | 0.6243 |
| | Ce4 O4 Se3 | 96-430-5045 | 0.6243 |
| Zn13 Ti66 Si100 Al92 O384 (Zn O)2 | Al92 O386 Si100 Ti66 Zn15 | 96-152-1493 | 0.6231 |
| Mg4.76Fe0.22Ti0.2Si1.99O8((H)1.26F0.74)(Natural chondrodite at 7.3 GPa) | F0.74 Fe0.22 H1.26 Mg4.76 O9.26 Si1.99 Ti0.02 | 96-154-4884 | 0.6230 |
| Spinel | Al0.988 Cr0.883 Fe0.469 Mg0.684 Mn0.005 Ni0.001 O4 Si0.003 Ti0.015 C4 H12 A15 F17 N10 | 96-900-4938 | 0.6227 |
| | | 96-450-6127 | 0.6224 |
| Catena-bis(tris(2-Amineoethy)amine-cadmium(ii)hexacyano-iron(ii)trihydrate | C99 Cd11 Fe10.5 N77 O33 | 96-700-9718 | 0.6216 |
| Manesiochromite | Al0.973 Cr0.973 Fe0.449 Mg0.684 Mn0.006 Ni0.001 O4 Si0.001 Ti0.003 Zn0.006 | 96-900-4939 | 0.6213 |
| Na2 Pt (O D)6 | D6 Na2 O6 Pt | 96-152-4014 | 0.6195 |
| Chromite | Al0.546 Cr0.422 Fe0.562 Mg0.457 Ni0.002 O4 Si0.002 Ti0.044 Zn0.007 | 96-900-4950 | 0.6191 |

And 516 others...

Search-Match

Settings

| | |
|--------------------------------------------|----------------------|
| Reference database used | COD-Inorg 2021.06.14 |
| Automatic zeropoint adaptation | Yes |
| Downgrade entries with low scaling factors | Yes |
| Minimum figure-of-merit (FoM) | 0.60 |
| 0.60 | |
| 2theta window for peak corr. | 0.30 deg. |
| Minimum rel. int. for peak corr. | 1 |
| Parameter/influence 2theta | 0.50 |
| Parameter/influence intensities | 0.50 |
| Parameter multiple/single phase(s) | 0.50 |

Criteria for entries added by user

Reference:

Entry number: 96-154-4616;96-154-4617;96-900-0167;96-900-0168;96-900-0168;96-900-0268;96-900-0315;96-900-0316;96-900-0317;96-900-0318;96-900-0319;96-900-0320;96-900-0321;96-900-0322;96-900-0323;96-900-0324;96-900-0325;96-900-0326;96-900-0327;96-900-0535;96-900-0536;96-900-0537;96-900-0538;96-900-0539;96-900-0540;96-900-0541;96-900-0542;96-900-0788;96-900-1667;96-900-1668;96-900-1669;96-900-1670;96-900-1671;96-900-4323;96-900-4324;96-900-4325;96-900-4326;96-900-4327;96-900-4328;96-900-4329;96-900-4330;96-900-4331;96-900-4332;96-900-4333;96-900-7378;96-901-0755;96-901-0756;96-901-0757;96-901-0758;96-901-0759;96-901-0760;96-901-0761;96-901-0762;96-901-0763;96-901-0764;96-901-0765;96-901-0766;96-901-0776;96-901-0777;96-901-0778;96-901-0779;96-901-0780;96-901-0781;96-901-1462;96-901-1463;96-901-1464;96-901-1465;96-901-1466;96-901-1467;96-901-1468;96-901-3094;96-901-3095;96-901-3096;96-901-3097;96-901-3098;96-901-3099;96-901-3100;96-901-3101;96-901-3102;96-901-3640;96-901-3641;96-901-3642;96-901-4298;96-901-5075;96-901-

5346;96-901-5659;96-901-6386;96-100-0048;96-101-1019;96-154-5543;96-154-8550;96-154-8551;96-154-8552;96-900-1179;96-900-1221;96-900-1594;96-900-1595;96-900-1596;96-900-1597;96-900-1598;96-900-1599;96-900-1600;96-900-1601;96-900-1602;96-900-1642;96-900-1643;96-900-1644;96-900-1645;96-900-1646;96-900-1700;96-900-1701;96-900-2711;96-900-2712;96-900-2713;96-900-2714;96-900-2715;96-900-2716;96-900-2717;96-900-4030;96-900-4031;96-900-4032;96-900-4033;96-900-4034;96-900-4118;96-900-4119;96-900-4957;96-900-4958;96-900-5542;96-900-5543;96-900-5544;96-900-5545;96-900-5589;96-900-5590;96-900-5776;96-900-5777;96-900-6338;96-900-6339;96-900-6340;96-900-6341;96-900-6342;96-900-6343;96-900-6428;96-900-6429;96-900-6430;96-900-6431;96-900-6432;96-900-6433;96-900-6434;96-900-6435;96-900-6436;96-900-6437;96-900-6438;96-900-6439;96-900-6440;96-900-6441;96-900-6442;96-900-6443;96-900-8078;96-900-8165;96-901-0242;96-901-0872;96-901-0873;96-901-0874;96-901-0888;96-901-0889;96-901-0890;96-901-0891;96-901-0892;96-901-0893;96-901-0894;96-901-0895;96-901-0896;96-901-0897;96-901-0898;96-901-0899;96-901-1582;96-901-3659;96-901-4118;96-901-4448;96-901-4536;96-901-4861;96-901-4978;96-901-4984;96-901-5810;96-901-6053;96-901-6154;96-901-6258;96-901-6266;96-901-6573;96-900-0849;96-900-1092;96-900-1093;96-900-1639;96-900-1640;96-900-1779;96-900-1883;96-900-4509;96-900-4510;96-900-4511;96-900-4512;96-900-4513;96-900-4514;96-900-4994;96-900-4995;96-900-7425;96-901-4665;96-901-5164;96-901-5487;96-901-5581;96-901-6051;96-901-6148;96-900-3104;96-900-4000;96-900-4515;96-901-4626;96-901-5975;96-901-6234;96-101-1153;96-300-0049;96-900-8041;96-900-8298;96-900-8732;96-901-4436;96-900-0097;96-900-0381;96-900-0972;96-900-0973;96-900-0974;96-900-0975;96-900-0976;96-900-1850;96-900-1851;96-900-1852;96-900-1853;96-900-1854;96-900-1855;96-900-2811;96-900-2812;96-900-2813;96-900-2814;96-900-2815;96-900-2816;96-900-2817;96-900-2818;96-900-2819;96-900-2820;96-900-2821;96-900-7693;96-900-9130;96-901-0201;96-901-0202;96-901-0203;96-901-0209;96-901-0210;96-901-0211;96-901-0214;96-901-0215;96-901-0216;96-901-0217;96-901-0218;96-901-0224;96-901-0225;96-901-0226;96-901-0227;96-901-1208;96-101-1098;96-101-1160;96-101-1173;96-101-1177;96-101-1201;96-110-0020;96-500-0036;96-900-0776;96-900-0777;96-900-0778;96-900-0779;96-900-

0780;96-900-0781;96-900-5018;96-900-5019;96-900-5020;96-900-5021;96-900-5022;96-900-5023;96-900-5024;96-900-5025;96-900-5026;96-900-5027;96-900-5028;96-900-5029;96-900-5030;96-900-5031;96-900-5032;96-900-5033;96-900-5034;96-900-7379;96-900-8093;96-900-8094;96-900-9667;96-901-0145;96-901-0146;96-901-0147;96-901-1494;96-901-1495;96-901-1496;96-901-1497;96-901-2601;96-901-2602;96-901-2603;96-901-2604;96-901-2605;96-901-2606;96-901-3322;96-901-5023;96-101-1033;96-101-1085;96-722-8111;96-900-0927;96-900-0928;96-900-0929;96-900-0930;96-900-0931;96-900-0932;96-900-0933;96-900-0934;96-900-0935;96-900-2317;96-900-2318;96-900-2319;96-900-2320;96-900-2321;96-900-2322;96-900-2323;96-900-2324;96-900-2325;96-900-2326;96-900-2327;96-900-2328;96-900-2329;96-900-2330;96-900-2331;96-900-2332;96-900-2333;96-900-2674;96-900-2675;96-900-4088;96-900-4156;96-900-4157;96-900-5813;96-900-5814;96-900-5815;96-900-5816;96-900-5817;96-900-5837;96-900-5838;96-900-5839;96-900-5840;96-900-5841;96-900-5842;96-900-5843;96-900-6185;96-900-6190;96-900-6195;96-900-6200;96-900-6243;96-900-6248;96-900-6253;96-900-6266;96-900-6921;96-900-6922;96-900-7645;96-900-7707;96-900-7708;96-900-9769;96-900-9770;96-901-0940;96-901-0941;96-901-0942;96-901-3530;96-901-3531;96-901-3532;96-901-3533;96-901-3534;96-901-3535;96-901-3536;96-900-6565;96-901-0767;96-901-0768;96-201-4615;96-900-0150;96-900-2481;96-900-2482;96-900-2483;96-900-2484;96-900-2485;96-900-2486;96-900-5435;96-100-8767;96-100-8768;96-100-8769;96-101-1088;96-221-1653;96-900-2159;96-900-2160;96-900-3077;96-900-3078;96-900-3079;96-900-3080;96-900-3081;96-901-0407;96-901-0408;96-901-0409;96-901-0410;96-901-0411;96-901-1413;96-901-5697;96-901-6060;96-901-6179;96-901-6407;96-100-0036;96-120-0007;96-900-1616;96-900-2902;96-900-5139;96-900-5844;96-900-9321;96-900-9665;96-900-7595

Peak List

| <i>N</i> <i>o.</i> | <i>2theta</i> [°] | <i>d</i> [Å] | <i>I/I0</i> (peak height) | <i>Counts</i> (peak area) | <i>FWHM</i> | <i>Matche</i> <i>d</i> |
|-----------------------|----------------------|--------------|------------------------------|------------------------------|-------------|---------------------------|
| 1 | 6.40 | 13.7993 | 512.34 | 59.72 | 1.0000 | A |
| 2 | 9.46 | 9.3415 | 148.93 | 5.55 | 0.3200 | A,D,E |
| 3 | 12.36 | 7.1554 | 1000.00 | 60.61 | 0.5200 | A,C |
| 4 | 18.66 | 4.7514 | 491.12 | 27.48 | 0.4800 | A |

| | | | | | | |
|----|-------|--------|--------|-------|--------|---------|
| 5 | 19.48 | 4.5532 | 337.43 | 20.45 | 0.5200 | A,C,D,E |
| 6 | 19.86 | 4.4669 | 270.40 | 40.34 | 1.2800 | A,D,E |
| 7 | 21.16 | 4.1953 | 548.16 | 66.45 | 1.0400 | A,B,D |
| 8 | 24.98 | 3.5618 | 844.37 | 47.24 | 0.4800 | A |
| 9 | 26.76 | 3.3287 | 570.29 | 21.27 | 0.3200 | A,B,E |
| 10 | 28.66 | 3.1122 | 409.24 | 13.36 | 0.2800 | A,D |
| 11 | 30.60 | 2.9192 | 177.62 | 7.45 | 0.3600 | A |
| 12 | 33.38 | 2.6822 | 227.19 | 27.54 | 1.0400 | A,B,C,D |
| 13 | 34.76 | 2.5788 | 362.48 | 27.04 | 0.6400 | A,B,D,E |
| 14 | 35.84 | 2.5035 | 654.70 | 85.47 | 1.1200 | A,B,C,E |
| 15 | 36.88 | 2.4353 | 631.90 | 55.97 | 0.7600 | A,B,D |
| 16 | 37.84 | 2.3757 | 148.39 | 6.92 | 0.4000 | A,D |
| 17 | 39.94 | 2.2555 | 170.85 | 50.98 | 2.5600 | A,B,D,E |
| 18 | 53.40 | 1.7144 | 248.69 | 31.31 | 1.0800 | B,D,E |
| 19 | 58.90 | 1.5667 | 179.38 | 10.04 | 0.4800 | C,D,E |
| 20 | 60.18 | 1.5364 | 304.64 | 22.72 | 0.6400 | C,D,E |
| 21 | 61.50 | 1.5066 | 222.98 | 27.03 | 1.0400 | B,C,D,E |

Integrated Profile Areas

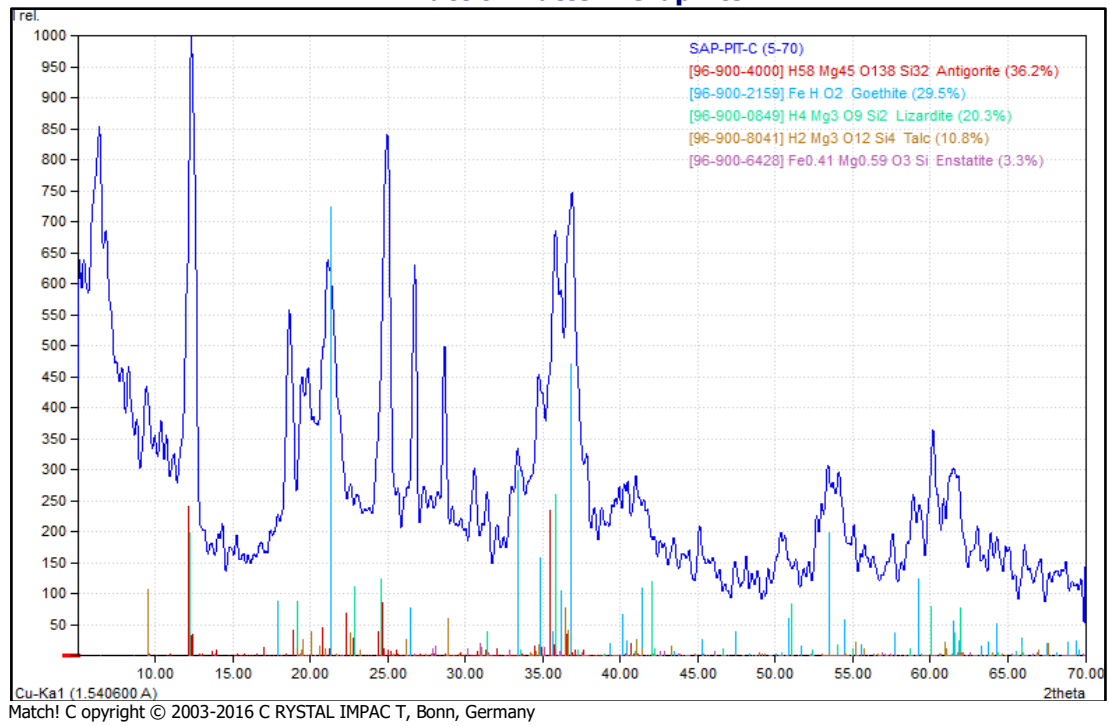
Based on calculated profile

| Profile area | Counts | Amount |
|------------------------------------------|---------------|---------------|
| Overall diffraction profile | 98147 | 100.00% |
| Background radiation | 59775 | 60.90% |
| Diffraction peaks | 38372 | 39.10% |
| Peak area belonging to selected phases | 24706 | 25.17% |
| <i>Peak area of phase A (Antigorite)</i> | <i>5623</i> | <i>5.73%</i> |
| <i>Peak area of phase B (Goethite)</i> | <i>10923</i> | <i>11.13%</i> |
| <i>Peak area of phase C (Lizardite)</i> | <i>4459</i> | <i>4.54%</i> |
| <i>Peak area of phase D (Talc)</i> | <i>2841</i> | <i>2.89%</i> |
| <i>Peak area of phase E (Enstatite)</i> | <i>859</i> | <i>0.88%</i> |
| Unidentified peak area | 13666 | 13.92% |

Peak Residuals

| Peak data | Counts | Amount |
|---------------------------------------------|---------------|---------------|
| Overall peak intensity | 715 | 100.00% |
| Peak intensity belonging to selected phases | 558 | 78.09% |
| Unidentified peak intensity | 157 | 21.91% |

Diffraction Pattern Graphics



LAMPIRAN D

HASIL ANALISIS *X-RAY FLOURESCENCE* (XRF)

| Identifikasi | Sequence | Time | Pos | Persentase Kadar (%) | | | | | | | |
|-----------------|----------|-----------------|-----|----------------------|-------|-------|-------|-------|------|------|------|
| | | | | Ni | Fe | Si | Mg | Al | Ca | Cr | Co |
| QS AA/ LIM PITC | 1 of 1 | 6/19/2021 11:30 | 2 | 0,95 | 35,76 | 33,51 | 10,28 | 10,34 | 0,06 | 2 | 0,07 |
| QS AA/ SAP PITC | 1 of 1 | 6/19/2021 11:30 | 3 | 1,59 | 32,94 | 36,03 | 8,22 | 8,85 | 0,09 | 2,12 | 0,06 |